Kobayashi et al., J Nanomater Mol Nanotechnol 2016, 5:4
DOI: 10.4172/2324-8777.1000191

Journal of Nanomaterials & Molecular Nanotechnology

Research Article

A SCITECHNOL JOURNAL

Preparation of a Colloid Solution of Au/Silica Core-Shell Nanoparticles Surface-Modified with Cellulose and its X-ray Imaging Properties

Yoshio Kobayashi[1]*, Ryoko Nagasu[1], Tomohiko Nakagawa[2], Yohsuke Kubota[2], Kohsuke Gonda[2] and Noriaki Ohuchi[2]

Abstract

Objective: The aim of this paper is to describe the preparation of a colloid solution of Au nanoparticles that are coated with silica and simultaneously surface modified with carboxymethylcellulose (CMC) (Au/SiO_2/CMC) and to investigate the X-ray imaging of mice using the colloid solution.

Methods: The reduction of Au ions (III) with sodium citrate produced Au nanoparticles, and amino groups were introduced on the surface of the Au nanoparticles by using (3-aminopropyl)-trimethoxysilane. The Au nanoparticles with amino groups were silica coated by a sol-gel process using tetraethylorthosilicate, (3-aminopropyl)-triethoxysilane, water and sodium hydroxide in ethanol (Au/SiO_2-NH_2). After concentrating the as-prepared Au/SiO_2-NH_2 particle colloid solution by centrifugation, CMC was immobilized on the Au/SiO_2-NH_2 particle surface with the addition of CMC to the Au/SiO_2-NH_2 particle colloid solution.

Results: The Au/SiO_2/CMC particles, with a size of 67.4 ± 5.4 nm containing a core of a single Au nanoparticle with a size of 17.9 ± 1.3 nm, were produced using the preparation conditions adopted in the present work. A computed tomography (CT) value that was as high as 344 ± 12 Hounsfield units (HU) was recorded for the Au/SiO_2/CMC particle colloid solution with an Au concentration of 0.043 M. Its converted value was calculated by dividing the Au concentration into the recorded CT value and was 8.0×10^3 HU/M. This value was larger than that of Iopamiron 300, a commercial X-ray contrast agent. The Au/SiO_2/CMC particle colloid solution was injected into the tail vein of a mouse and could be used to image the tissues.

Conclusion: The Au/SiO_2/CMC particle colloid solution obtained in the present work was successfully used for X-ray imaging.

Keywords

Au; Silica; Core-shell; Nanoparticle; Colloid; Carboxymethylcellulose; X-ray imaging; X-ray contrast agent

Introduction

The imaging technique of using X-rays is one of the representative techniques for medical diagnosis [1-3] and has become indispensable to modern medical diagnosis. The use of contrast agents in the X-ray imaging process makes X-ray images clear [3]. Typically, commercially available X-ray contrast agents are solutions of iodine complexes. They have been used in the X-ray imaging process for many years [4-8] because they function well as an X-ray contrast agent. However, some problems have been identified with using the iodine-based contrast agents. One problem is related to their residence time in living bodies, which some researchers have noted [9-11]. Because iodine compounds are present in solution at the molecular size range, the viscous resistance of body fluid does not act strongly on the iodine compounds in living bodies. As a result, the iodine compounds move fast, and then cannot reside in the living body for a long time. This makes it difficult to obtain clear and steady X-ray images using commercial X-ray contrast agents. To increase the residence time of contrast agents, the formation of nanometer-sized particles containing contrast chemicals may be effective because of the viscous resistance of a fluid acting on particles larger than the contrast chemicals in the molecular size range. The other problem concerns the adverse events derived from the iodine compounds [12-14]. Some patients suffer from adverse events such as allergic reactions to iodine compounds.

Apart from the iodine-based contrast agents, Au also has the ability to increase the contrast of X-ray images because of its strong absorption of X-rays. In addition, nanoparticles of metallic Au can be easily produced by methods such as the reduction of Au ions with a reducing reagent, such as citric acid or L-ascorbic acid. The Au nanoparticles are expected to be acted upon strongly by viscous resistance compared with the iodine compounds in the molecular size range. Based on their absorption ability and particle formation, nanoparticle colloid solutions of metallic Au have been examined as X-ray contrast agents to image tissues in living bodies at the nanometer scale [15-17]. The toxicity of ions released from metallic gold has been noted by several researchers [18-20], although it is not serious compared with that of the iodine compounds. The toxicity of both contrast agent materials arises from their direct contact with living bodies. A promising method to control direct contact is to coat the Au nanoparticles with materials with a lower toxicity. A possible example is particles with a core-shell structure composed of an Au-particle core and a silica shell. The toxicity of the Au particles should be reduced because the silica shell eliminates the contact between the Au particles and the living body. Various techniques for the silica coating of Au particles have been proposed in previous decades and in recent years [21-26]. In most techniques, (1) the Au nanoparticle colloid solution is prepared, (2) the affinity of the Au surface towards a silica source, such as alkoxide groups, is increased by surface modifying the Au nanoparticles, and (3) the silica shells are produced on the surface-modified Au particles through a sol-gel reaction of the silicon alkoxide. Our research group has also proposed a method to fabricate silica-coated Au nanoparticles (Au/SiO_2) [27-33]. Living bodies recognize the hydrophobic material as foreign, which decreases their blood circulation and residence in living bodies [34-36]. Thus, the surface modification of the particle with hydrophilic materials is a promising technique. Poly(ethylene glycol) (PEG) is often used as an agent for surface modification because it has multiple hydrophilic groups in its structure [34-38]. A PEG that has functional groups such as silicone alkoxide and pyrrolidinyl groups can be used for efficient

***Corresponding author:** Yoshio Kobayashi, Department of Biomolecular Functional Engineering, College of Engineering, Ibaraki University, 4-12-1 Naka-narusawa-cho, Hitachi, Ibaraki 316-8511, Japan, Fax: +81-294-38-5078; Tel: +81-294-38-5052; E-mail: yoshio.kobayashi.yk@vc.ibaraki.ac.jp

Received: June 21, 2016 **Accepted:** August 08, 2016 **Published:** August 14, 2016

surface modification. However, such PEGs with functional groups are costly compared with the functional group-free PEG. CMC is one of the representative hydrophilic polymers. Because CMC has carboxyl groups, it will be efficiently immobilized on a particle surface with amino groups.

The present work proposes a method to produce Au/SiO_2 particles with their surface modified by CMC (Au/SiO_2/CMC). To perform an efficient modification of the silica surface of the Au/SiO_2 particles with CMC, amino groups were immobilized on the Au/SiO_2 particles by the simultaneous formation of the silica shell and surface amination, which has been developed in our previous work [31]. The surface modification with CMC was performed by simply adding the CMC to the aminated Au/SiO_2 particle colloid solution. The suitability for X-ray imaging of the Au/SiO_2/CMC particle colloid solution was also investigated in the present work: the X-ray absorption of the Au/SiO_2/CMC particle colloid solution was measured, and the tissues of a mouse, into which the particle colloid solution was injected, were imaged.

Experimental Materials and Methods

Materials

Hydrogen tetrachloroaurate (III) trihydrate ($HAuCl_4 \cdot 3H_2O$) (Kanto Chemical, 98%) and trisodium citrate dihydrate (Na-cit) (Kanto Chemical, 99%) were used as an Au source and a reducing reagent to fabricate Au nanoparticles, respectively. The silane coupling agent used to increase the affinity between the Au particle surface and the silica shell was (3-aminopropyl)trimethoxysilane (APMS) (Sigma-Aldrich, 97%). For the silica coating, tetraethylorthosilicate (TEOS) (Kanto Chemical, 95%), a NaOH aqueous solution (Kanto Chemical, 1 M), APMS and ethanol (Kanto Chemical, 99.5%) were used as a silica source, a catalyst for the sol-gel reaction of TEOS, a silica source with an amino group and a solvent, respectively. CMC was used to modify the particle surface. All of the chemicals were used as received. Water was ion-exchanged and distilled using a Yamato WG-250 for use in the preparation.

Preparation

A colloid solution of Au nanoparticles was prepared by adding an Na-cit aqueous solution to an $HAuCl_4$ aqueous solution under vigorous stirring at 80°C. Our previous work showed that the colloid solution prepared with initial concentrations of 2.4×10^{-4} M Au and 1.6×10^{-3} M Na-cit had a surface plasmon resonance peak at 520.5 nm, and the average Au nanoparticle size was 17.9 ± 1.3 nm [31].

The silica coating and the introduction of amino groups onto the surface of the silica-coated particles were sequentially performed with a sol-gel process using TEOS and APMS, according to our previous work [31]. The obtained Au nanoparticle colloid solution and an APMS/ethanol solution were sequentially added to H_2O/ethanol. After 15 min, a TEOS/ethanol solution was added to the colloid solution. After another 15 min, an NaOH aqueous solution was rapidly injected into the Au/TEOS/H_2O/ethanol colloid solution to initiate the sol-gel reaction of TEOS. After another 15 min, an APMS/ethanol solution was added to the mixture to initiate the sol-gel reaction of the newly added APMS, which gave the aminated Au/SiO_2 particles (as-prepared Au/SiO_2-NH_2). The reaction temperature and time were 35°C and 24 h, respectively. The initial concentrations of Au, APMS (for the first addition), APMS (for the second addition), NaOH, H_2O, and TEOS in the as-prepared Au/SiO_2-NH_2 particle colloid solution were adjusted to 4.3×10^{-5}, 2×10^{-5}, 1.0×10^{-4}, 5.0×10^{-4}, 10.7, and 5.0×10^{-4} M, respectively. The as-prepared Au/SiO_2-NH_2 particles were washed and concentrated by repeating the following process three times: centrifugation of the Au/SiO_2-NH_2 particle colloid solution at ca. 18000 rev/min for ca. 30 min, removal of the supernatant with decantation, addition of the solvent and shaking of the colloid solution with a vortex mixer (concentrated Au/SiO_2-NH_2 particles). Ethanol was used as the solvent in the first process, and water was used as the solvent in the second and third processes. Finally, the as-prepared Au/SiO_2-NH_2 particle colloid solution was concentrated to 1/2000 by decreasing the amounts of added solvent.

The immobilization of CMC on the particle surface was performed by utilizing the electrostatic interaction between the cationic surface of the amino groups on the Au/SiO_2-NH_2 particles and the carboxyl groups (anions) of CMC. Equal volume portions of a 2 g/L CMC aqueous solution and the concentrated Au/SiO_2-NH_2 particle colloid solution were combined to immobilize CMC on the particle surface (Au/SiO_2/CMC), which diluted the initial Au nanoparticle colloid solution to 1/1000 in the Au/SiO_2/CMC particle colloid solution by volume. Consequently, the Au concentration in the final Au/SiO_2/CMC particle colloid solution was expected to be 0.043 M, if the entire $HAuCl_4$ was reduced to form Au nanoparticles and no particles were lost during the washing process.

Characterization

The samples were characterized using visible (VIS) spectroscopy, dynamic light scattering (DLS) and transmittance electron microscopy (TEM). The VIS extinction of the particle colloid solution was measured using a Shimadzu UV-3101PC spectrophotometer. The distribution of particle size was measured using DLS. The DLS was performed using a Malvern ZS90 particle size and zeta potential analyzer. The TEM was performed using a JEOL JEM-2100 microscope that operated at 200 kV. The TEM samples were prepared by dropping and evaporating the nanoparticle suspensions on a colloid-coated copper grid. Dozens of particle diameters were measured to determine the volume averaged particle size.

CT images and CT values of samples were obtained using an Aloka La theta LCT-200 CT system, which was also used in our previous works [29,30]. The samples were the Au/SiO_2/CMC particle colloid solution and an imprinting control region mouse with an age of 5-6 weeks. The colloid solution was injected into the tail vein of the mouse under anesthesia. The sample was placed in a tube with a diameter of 3.7 cm and a length of 29.5 cm. The images were taken as if the samples were cut into round slices. The CT values were estimated based on the CT values of -1000 and 0 Hounsfield units (HU) for air and water, respectively.

Results and Discussion

Specifications of Au/SiO_2/CMC particles

Figure 1 (a) shows a photograph of the concentrated Au/SiO_2/CMC particle colloid solution. The concentrated colloid solution is dark red in color. Although the particle colloid solution was concentrated to 1/1000 of the volume of the as-prepared Au nanoparticle colloid solution during the preparation, it was confirmed by the naked eye that the dark red colloid solution contained no sediment. This confirmation indicated that the Au/SiO_2/CMC particle colloid solution was colloidally stable at the micrometer-meter order, even at a high concentration.

An inset of Figure 2 shows a photograph of the Au/SiO_2/CMC particle colloid solution, which was prepared by diluting the

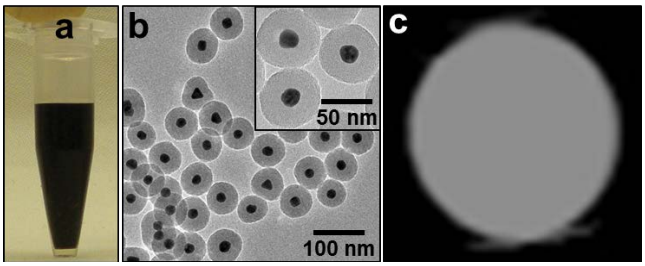

Figure 1: Images of Au/SiO_2/CMC particles. Images (a), (b) and (c) are a photograph of concentrated Au/SiO_2/CMC colloid solution, a TEM image of Au/SiO_2/CMC particles in the concentrated colloid solution, and a CT image of the concentrated colloid solution, respectively.

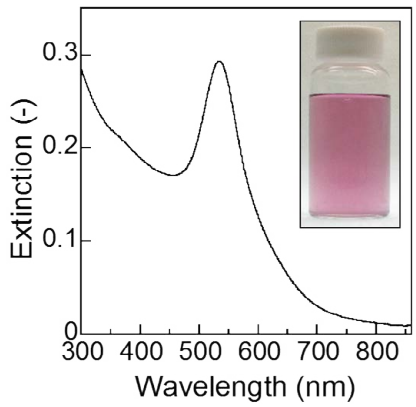

Figure 2: UV-VIS extinction spectrum of Au/SiO_2/CMC particle colloid solution. Inset shows its photograph.

concentrated Au/SiO_2/CMC particle colloid solution for measuring its VIS extinction spectrum. The colloid solution had a color of purple. This color appeared to be derived from the surface plasmon resonance absorption of the metallic Au nanoparticles. Figure 2 shows a VIS extinction spectrum of the colloid solution. The surface plasmon band was observed at 534.0 nm. The surface plasmon band red-shifted slightly with respect to the uncoated Au nanoparticles. The red shift of the plasmon band is due to a local increase of the refractive index around the Au particles [39]. A similar mechanism was also considered in the present work. Accordingly, this result implied that the Au nanoparticles were coated with silica, and the core-shell structure was maintained even after the processes of immobilizing the CMC and concentrating the Au/SiO_2/CMC particle colloid solution. In addition to the surface plasmon band, no surface plasmon band was observed at a wavelength longer than ca. 600 nm. This result indicated that the Au nanoparticles did not aggregate because the aggregation of Au nanoparticles causes their surface plasmon band to be detected at longer wavelengths. The maintenance of the core-shell structure prevented the Au nanoparticles from aggregating because of the physical barrier of the silica shells.

Figure 1 (b) shows a TEM image of the Au/SiO_2/CMC particles. Most of the particles observed in the image contained a single core of consisting of a Au nanoparticle. Accordingly, this observation also supported the maintenance of core-shell structure. Their particle size (TEM particle size) was 67.4 ± 5.4 nm. Figure 3 shows the particle size distribution of the Au/SiO_2/CMC particles. The particle sizes were in the range of 30-200 nm, and the particle size that gave the largest distribution (DLS particle size) was 61.2 nm. This DLS particle size corresponded with the TEM particle size. This correspondence reconfirmed that most of the produced particles had the core-shell structure observed in Figure 1 (b).

X-ray imaging

Figure 1 (c) shows a CT image of the Au/SiO_2/CMC particle colloid solution. The image was clear with a light contrast, and its CT value was as high as 344 ± 12 HU. This value was converted to a value with respect to the molar concentration of subject materials such as Au and I (converted CT value) to compare with the CT value of the commercial contrast agent. The converted CT value was 8.0×10^3 HU/M because of the Au concentration of 0.043 M. According to our previous work, a converted CT value of Iopamiron 300 with respect to the iodine concentration is 4.76×10^3 HU/M [30]. The converted CT value of the Au/SiO_2/CMC particle colloid solution was 1.7 times larger than that of Iopamiron 300. Gold absorbs X-rays more strongly than iodine per atom because of its large atomic number. Accordingly, the Au/SiO_2/PEG particle colloid solution had a large converted CT value. Thus, this result indicated that the Au/SiO_2/CMC particle colloid solution could function as an X-ray contrast agent for sensitivity.

Figure 4 shows the X-ray images of the mouse before and after it was injected with the Au/SiO_2/CMC particle colloid solution. Figure 5 shows the CT values of the various tissues as a function of time after the injection, where a value at 0 min indicated that it was prior to the injection. For a kidney, the contrast was not remarkably changed, and its CT value was nearly constant at approximately 60 HU. After the injection, the contrast of the liver and the spleen appeared to be slightly lighter than prior to the injection. Their CT values were 84.5 and 83.0 HU prior to the injection, respectively. The values jumped to 118.0 HU at 5 min after the injection and then almost leveled off. The Au/SiO_2/PEG particles were trapped and accumulated in the liver and the spleen immediately after the injection. As a result, the jump and the level-off were observed for the CT values of the liver and the spleen. For the heart, the injection also provided no remarkable change in contrast, which indicated that the Au/SiO_2/CMC particles had been trapped and had subsequently accumulated, and the particles were not circulated in the mouse. A similar result was also obtained in our previous studies on Au/SiO_2 particle colloid solutions [30,33]. The effect of CMC immobilization on the particles with regard to the circulation did not appear contrary to our expectation, which meant

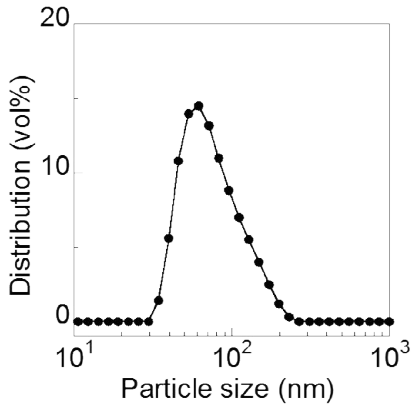

Figure 3: Particle size distribution of Au/SiO_2/CMC particles.

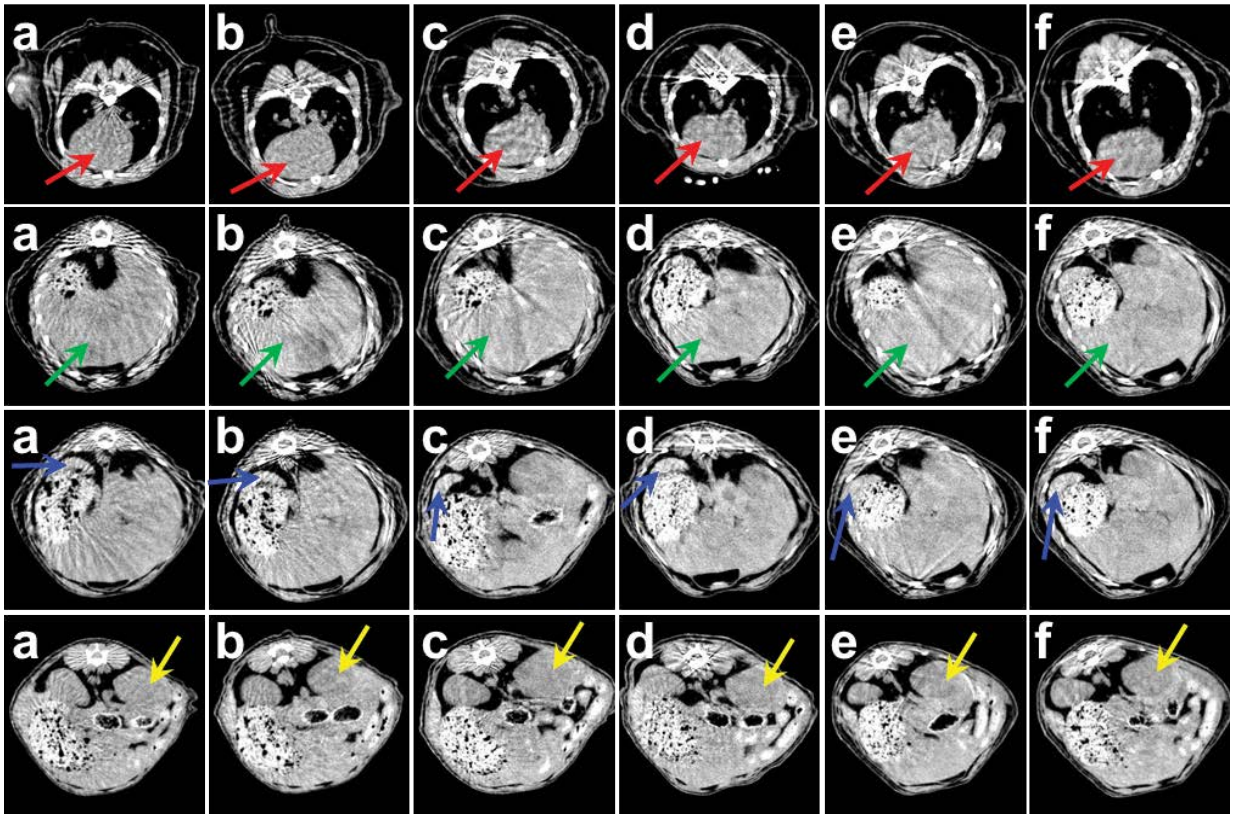

Figure 4: CT images of the heart (red arrows), liver (green arrows), spleen (blue arrows) and kidney (yellow arrows) of the mouse after injecting concentrated Au/SiO_2/CMC colloid solution. The images were taken (a) before injection and at (b) 5, (c) 60, (d) 180, (e) 360, and (f) 720 min after injection.

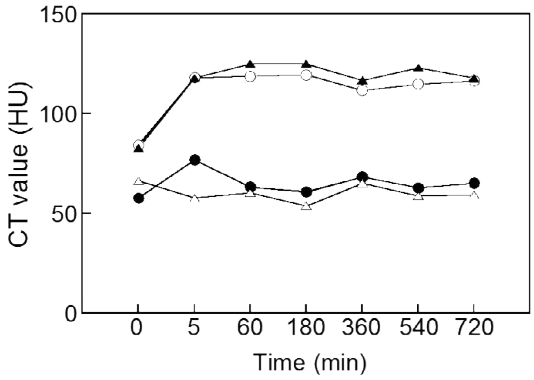

Figure 5: CT values of the heart (closed circles), liver (open circles), spleen (closed triangles) and kidney (open triangles) of a mouse after the injection of concentrated Au/SiO_2/CMC colloid solution.

that the CMC could not increase the circulation time. Another reason was considered as follows. The carboxyl group of CMC was expected to react with the amino group on particles to form a peptide bond, which immobilizes CMC on the particle surface. However, the CMC immobilization did not take place efficiently in the present work, although the reason remains unclear. Thus, only a small amount of CMC was immobilized on the particle surface. Consequently, the CMC could not increase the overall circulation time because of the small amount that was immobilized.

Conclusions

Au/SiO_2-NH_2 particles that contained Au cores with a size of 17.9 ± 1.3 nm were fabricated by the simultaneous synthesis of silica-coated Au nanoparticles and the introduction of amino groups to the Au/SiO_2 particles during silica coating. The particles of the colloid solution of Au/SiO_2/CMC were produced with a size of 67.4 ± 5.4 nm by allowing the CMC to react with the amino groups on the Au/SiO_2-NH_2 particles. The Au/SiO_2/CMC particle colloid solution could absorb X-rays better than the commercial X-ray

contrast agent: the Au/SiO_2/CMC particle colloid solution had a CT value of 8.0×10^3 HU/M (with respect to the Au concentration), which is higher than that of the commercial X-ray contrast agent. The injection of the Au/SiO_2/CMC particle colloid solution into a mouse lightened the contrast of its internal organs, i.e., increased their CT values. Accordingly, the Au/SiO_2/CMC particle colloid solution was applicable as an X-ray contrast agent. Because this paper focused on the time dependence of the CT values of various tissues in the mouse, other parameters, such as the toxicity of the particle colloid solution and the precise mechanisms of amination and CMC immobilization, were not investigated. Further studies on the parameters such as the toxicity of the particle colloid solutions, the precise mechanisms of CMC immobilization and the efficient immobilization of CMC are required in the next steps toward practical use.

Acknowledgments

We express our thanks to Prof. T. Noguchi at the College of Science of Ibaraki University, Japan (current affiliation: Faculty of Arts and Science of Kyushu University, Japan) for his help with the TEM observation. This work was supported by a Grant-in-Aid for Scientific Research on Innovative Areas "Nanomedicine Molecular Science" (No. 2306) from the Ministry of Education, Culture, Sports, Science, and Technology of Japan and by JSPS KAKENHI Grant Number 24310085.

References

1. Tsuji K, Nakano K, Hayashi H, Hayashi K, Ro CU (2008) X-ray spectrometry. Anal Chem 80: 4421-4454.
2. Liu Y, Al K, Lu L (2012) Nanoparticulate X-ray computed tomography contrast agents: From design validation to in vivo applications. Accounts Chem Res 45: 1817-1827.
3. Lusic H, Grinstaff MW (2013) X-ray-computed tomography contrast agents. Chem Rev 113: 1641-1666.
4. Numata K, Fukuda H, Morimoto M, Kondo M, Nozaki A, et al. (2012) Use of fusion imaging combining contrast-enhanced ultrasonography with a perflubutane-based contrast agent and contrast-enhanced computed tomography for the evaluation of percutaneous radiofrequency ablation of hypervascular hepatocellular carcinoma. Eur J Radiol 81: 2746-2753.
5. Takizawa H, Kondo K, Toba H, Kajiura K, Ali AHK, et al. (2012) Computed tomography lymphography by transbronchial injection of iopamidol to identify sentinel nodes in preoperative patients with non-small cell lung cancer: A pilot study. J Thorac Cardiovasc Surg 144: 94-99.
6. Yin WH, Lu B, Gao JB, Li PL, Sun K, et al. (2015) Effect of reduced x-ray tube voltage, low iodine concentration contrast medium, and sinogram-affirmed iterative reconstruction on image quality and radiation dose at coronary CT angiography: Results of the prospective multicenter. J Cardiovasc Comput Tomogr 9: 215-224.
7. Kitajima K, Ueno Y, Suzuki K, Kita M, Ebina Y, et al. (2012) Low-dose non-enhanced CT versus full-dose contrast-enhanced CT in integrated PET/CT scans for diagnosing ovarian cancer recurrence. Eur J Radiol 81: 3557-3562.
8. Koda M, Mandai M, Matono T, Sugihara T, Nagahara T, et al. (2010) Assessment of the ablated area after radiofrequency ablation by contrast-enhanced sonography; comparison with virtual sonography with magnetic navigation. Clin Imag 34: 60-64.
9. Hallouard F, Briancon S, Anton N, Li X, Vandamme T, et al. (2013) Iodinated nano-emulsions as contrast agents for preclinical X-ray imaging: Impact of the free surfactants on the pharmacokinetics. Eur J Pharm Biopharm 83: 54-62.
10. Jin E, Lu ZR (2014) Biodegradable iodinated polydisulfides as contrast agents for CT angiography. Biomater 35: 5822-5829.
11. Qiao Z, Shi X (2015) Dendrimer-based molecular imaging contrast agents. Prog Polym Sci 44: 1-27.
12. Thomsen HS (2011) Contrast media safety-An update. Eur J Radiol 80: 77-82.
13. Ares JDA, Amatriain GR, Iglesias CN, Forner MB, Gay MLF (2014) Contrast agents used in interventional pain: Management, complications, and troubleshooting. Tech Reg Anesth Pain Manag 18: 65-75.
14. Matsushita T, Kobayashi N, Hashizuka M, Sakuma H, Kondo T, et al. (2015) Changes in mutagenicity and acute toxicity of solutions of iodinated X-ray contrast media during chlorination. Chemosphere 135: 101-107.
15. Tu SJ, Yang PY, Hong JH, Lo CJ (2013) Quantitative dosimetric assessment for effect of gold nanoparticles as contrast media on radiotherapy planning. Radiat Phys Chem 88: 14-20.
16. Cole LE, Vargo-Gogola T, Roeder RK (2014) Bisphosphonate-functionalized gold nanoparticles for contrast-enhanced X-ray detection of breast microcalcifications. Biomater 35: 2312-2321.
17. Silvestri A, Polito L, Bellani G, Zambelli V, Jumde RP, et al. (2015) Gold nanoparticles obtained by aqueous digestive ripening: Their application as X-ray contrast agents. J Colloid Interface Sci 439: 28-33.
18. Otomo PV, Wepener V, Maboeta MS (2014) Single and mixture toxicity of gold nanoparticles and gold (III) to *Enchytraeus buchholzi* (Oligochaeta). Appl Soil Ecol 84: 231-234.
19. Rachmawati D, Alsalem IWA, Bontkes HJ, Verstege MI, Gibbs S, et al. (2015) Innate stimulatory capacity of high molecular weight transition metals Au (gold) and Hg (mercury). Toxicol in Vitro 29: 363-369.
20. Sathishkumar M, Pavagadhi S, Mahadevan A, Balasubramanian R (2015) Biosynthesis of gold nanoparticles and related cytotoxicity evaluation using A549cells. Ecotoxicol Environ Safe 114: 232-240.
21. Lee HB, Yoo YM, Han YH (2006) Characteristic optical properties and synthesis of gold-silica core-shell colloids. Scripta Mater 55: 1127-1129.
22. Zhang K, Wang W, Cheng W, Xing X, Mo G, et al. (2010) Temperature-induced interfacial change in $Au@SiO_2$ core-shell nanoparticles detected by extended X-ray absorption fine structure. J Phys Chem C 114: 41-49.
23. Wu Z, Liang J, Ji X, Yang W (2011) Preparation of uniform $Au@SiO_2$ particles by direct silica coating on citrate-capped Au nanoparticles. Colloids Surf A 392: 220-224.
24. Chang B, Zhang X, Guo J, Sun Y, Tang H, et al. (2012) General one-pot strategy to prepare multifunctional nanocomposites with hydrophilic colloidal nanoparticles core/mesoporous silica shell structure. J Colloid Interface Sci 377: 64-75.
25. Törngren B, Akitsu K, Ylinen A, Sandén S, Jiang H, et al. (2014) Investigation of plasmonic gold-silica core-shell nanoparticle stability in dye-sensitized solar cell applications. J Colloid Interface Sci 427: 54-61.
26. Raj S, Adilbish G, Lee JW, Majhi SM, Chon BS, et al. (2014) Fabrication of $Au@SiO_2$ core–shell nanoparticles on conducting glass substrate by pulse electrophoresis deposition. Ceram Int 40: 13621-13626.
27. Kobayashi Y, Inose H, Nakagawa T, Gonda K, Takeda M, et al. (2011) Control of shell thickness in silica-coating of Au nanoparticles and their X-ray imaging properties. J Colloid Interface Sci 358: 329-333.
28. Kobayashi Y, Inose H, Nakagawa T, Gonda K, Takeda M, et al. (2012) Synthesis of Au-silica core-shell particles by a sol-gel process. Surf Eng 28: 129-133.
29. Kobayashi Y, Inose H, Nakagawa T, Kubota Y, Gonda K, et al. (2013) X-ray imaging technique using colloid solution of Au/silica core-shell nanoparticles. J Nanostruct Chem 3: 62.
30. Kobayashi Y, Inose H, Nagasu R, Nakagawa T, Kubota Y, et al. (2013) X-ray imaging technique using colloid solution of Au/silica/poly(ethylene glycol) nanoparticles. Mater Res Innov 17: 507-514.
31. Kobayashi Y, Nagasu R, Shibuya K, Nakagawa T, Kubota Y, et al. (2014) Synthesis of a colloid solution of silica-coated gold nanoparticles for X-ray imaging applications. J Nanoparticle Res 16: 2551.
32. Kobayashi Y, Nagasu R, Nakagawa T, Kubota Y, Gonda K, et al. (2015) Preparation of Au/silica/poly(ethylene glycol) nanoparticle colloid solution and its use in X-ray imaging process. Nanocomposites 2: 83-88.
33. Kobayashi Y, Shibuya K, Tokunaga M, Kubota Y, Oikawa T, et al. (2016) Preparation of high-concentration colloidal solution of silica-coated gold nanoparticles and their application to X-ray imaging. J Sol-Gel Sci Technol 78: 82-90.

34. Parveen S, Sahoo SK (2011) Long circulating chitosan/PEG blended PLGA nanoparticle for tumor drug delivery. Eur J Pharmacol 670: 372-383.

35. Zamani S, Khoee S (2012) Preparation of coreeshell chitosan/PCL-PEG triblock copolymer nanoparticles with ABA and BAB morphologies: Effect of intraparticle interactions on physicochemical properties. Polymer 53: 5723-5736.

36. Khalil NM, Nascimento TCF, Casa DM, Dalmolin LF, Mattos AC, et al. (2013) Pharmacokinetics of curcumin-loaded PLGA and PLGA-PEG blend nanoparticles after oral administration in rats. Colloids Surf B 101: 353-360.

37. Illés E, Tombácz E, Szekeres M, Tóth IY, Szabó Á, et al. (2015) Novel carboxylated PEG-coating on magnetite nanoparticles designed for biomedical applications. J Mag Mag Mater 380: 132-139.

38. Hałupka-Bryl M, Bednarowicz M, Dobosz B, Krzyminiewski R, Zalewski T, et al. (2015) Doxorubicin loaded PEG-b-poly(4-vinylbenzylphosphonate) coated magnetic iron oxide nanoparticles for targeted drug delivery. J Mag Mag Mater 384: 320-327.

39. Liz-Marzán LM, Giersig M, Mulvaney P (1996) Synthesis of nanosized gold-silica core-shell particles. Langmuir 12: 4329-4335.

Author Affiliation

Top

[1]*Department of Biomolecular Functional Engineering, College of Engineering, Ibaraki University, 4-12-1 Naka-narusawa-cho, Hitachi, Ibaraki 316-8511, Japan*

[2]*Graduate School of Medicine, Tohoku University, Seiryo-machi, Aoba-ku, Sendai, Miyagi 980-8574, Japan*